Robust generation of relativistic mirrors from laser wakefields for enhanced laser backscattering

Jie Mu, Fei-Yu Li, Ming Zeng, Min Chen, and Jie Zhang
Key Laboratory for Laser Plasmas (MoE) and Department of Physics and Astronomy, Shanghai Jiao Tong University, Shanghai 200240, China

Zheng-Ming Sheng*
Key Laboratory for Laser Plasmas (MoE) and Department of Physics and Astronomy, Shanghai Jiao Tong University, Shanghai 200240, China and SUPA, Department of Physics, University of Strathclyde, Glasgow G4 0NG, UK
(Dated: November 13, 2013)

By adopting an up-ramp density profile, we propose to generate relativistic electron mirrors from laser-driven underdense plasma waves, which are insensitive to finite thermal temperature in certain range. Along the density ramp, premature plasma wave-breaking due to thermal effects is shown to be well mitigated, and overcritical dense electron sheets can pile up when approaching the end of the up-ramp. The consequent mirror speed can be stably driven to the group velocity of the laser propagating in a corresponding homogeneous plasma. Such a mirror is suitable for coherent backscattering of a counter-propagating probe pulse with increased stability and enhanced efficiency as compared with that produced in homogeneous plasma. Mirror reflectivity as high as a few percent for the field amplitude is identified through multi-dimensional particle-in-cell simulations.

Ultrashort coherent extreme-ultraviolet (XUV) or soft x-ray pulses have been demonstrated to be advanced tools both in fundamental research and for novel applications such as ultrafast imaging using pump-probe scenarios. Various methods for producing such pulses have been discovered, relying on either atomic or plasma processes [1]. In laser-plasma based x-rays sources, a very efficient configuration is to drive relativistic electron sheets for coherent pulse backscattering, where the scattered wave would gain both temporal compression and spectral upshifts by giant factors $4\gamma_x^2$ with $\gamma_x = 1/\sqrt{1-v_x^2/c^2}$ and v_x the normal velocity of the sheets [2]. For example, by focusing ultraintense few-cycle lasers onto a solid nanofoil, dense electron sheets can be blown out [3], and recent experiments have shown that an effective boost factor of $\gamma_x \simeq 2$ can be extracted for driver intensities at $6\times10^{20}\mathrm{W/cm^2}$ [4].

Another novel idea, first suggested by Bulanov *et al.*, is to treat the nonlinear density waves driven by an ultrashort intense laser in underdense plasmas as flying mirrors [5]. As compared to laser-foil scenarios, this scheme demands relatively gentle drive lasers [6, 7], and can be potentially operated at a high repetition rate using gas targets. In order to create such mirrors for efficient backscattering, it is crucial to drive the plasma waves closely to the wavebreaking point, where the maximal electron fluid velocity v_m matches with the phase velocity v_p of the wakefields. The density wave crests then develop singular spikes, leading to efficient scattering of a counter-propagating probe laser with Doppler upshifting factors $4\gamma_x^2 \simeq 4\gamma_p^2$. Here, $\gamma_p = 1/\sqrt{1-v_p^2/c^2}$ approximates to ω_L/ω_p in the linear regime with ω_L and ω_p the frequency of the drive laser and the plasma electrons, respectively. It is obvious that a sufficient intense laser can be used to drive v_m to v_p. Recently, a different method that enables gradual decline of v_p by adopting downward density transitions has been suggested which, however, provides even lower γ_x [8]. On the other hand, the spike singularity is very sensitive to the difference $v_m - v_p$, which is actually rather difficult to control in experiments. Despite all these, another major concern that has been neglected so far is the plasma thermal effect. It has been shown that finite thermal motion associated with the plasma electrons would broaden the spike singularities due to premature thermal injection, limit the singular status within a short time period and, as a consequence, significantly degrade the performance of such flying mirrors [9].

In this Letter, we address these issues by proposing wakefield excitation along an up-ramp density profile. The key element is that an up-ramp profile with proper density gradient will completely prevent premature wavebreaking even if finite plasma temperature is introduced. Due to the nonlinear wake evolution, overcritical dense wake spikes can be created for a sufficient long lifetime when approaching the end of the up-ramp. As tested by scattering of a probe laser pulse, the relativistic mirrors produced this way can result in efficient generation of attosecond XUV pulses as compared to those produced in uniform but thermal plasmas.

As shown before, tailoring plasma density is useful for laser wakefield accelerations such as density-gradient injection using a downward transition [10, 11]. Moreover, an up-ramp profile leads to some intriguing features for wakefield excitation since the wake wavelength stretches and contracts along the ramp. The former leads to the occurrence of linear mode conversion of electrostatic wakefields to electromagnetic emissions under

* zmsheng@sjtu.edu.cn

certain conditions [12]. The latter has been adopted to relieve the dephasing problem in electron acceleration by stabilizing the phase of injected beams with respect to the accelerating wave [13, 14]. Generally in the one-dimensional (1D) geometry, the normalized phase velocity of the wakefield at distance ξ behind the drive laser can be expressed as $\beta_p(x) = \beta_g/[1 - (\xi/2n)(dn/dx)]$. Here $\beta_g(x) \simeq \sqrt{1 - n(x)/n_c}$ describes the linear group velocity of the laser pulse at each density $n(x)$ along the propagation axis x. n_c is the critical electron density. It has been recently pointed out that β_p can exceed unity along the up-ramp, provided the density gradient satisfies $dn/dx > (1 - \beta_g)2n/\xi$. This marks a new feature of the up-ramp, and has been used for controlled generation of attosecond electron beams via a sharp transition of β_p [15]. The superluminality of β_p is crucial in the present scheme since it would completely suppress 1D wave breaking even for thermal plasmas with arbitrary intense drivers, thus may ultimately result in stable generation of relativistic mirrors in the wakefield.

We start by showing the 1D wakewave evolution along the up-ramp density profile and corresponding coherent backscattering using the particle-in-cell (PIC) code OSIRIS [16]. An inhomogeneous plasma density with a normal Gaussian profile $n(x) = n_0 e^{-(x-x_0)^2/L^2}$ is used as shown in Fig. 1(a), $n_0 = 0.04 n_c$ defines the peak density at the profile center $x_0 = 100\lambda_L$ with λ_L the laser wavelength. A scale length $L = 45\lambda_L$ is used, and longer scale lengths generally lead to few differences if only the density-gradient requirement given above is met. A linearly z-polarized drive pulse, starting at $x = -5\lambda_L$, impinges onto the plasma from the left with normalized vector potential $a = a_d \sin^2(\pi t/\tau_d)$. We take $a_d = 5.4$ corresponding to a peak intensity of $\sim 4 \times 10^{19}\mathrm{W/cm^2}$ at $\lambda_L = 1\mu$m, and $\tau_d = 13.2T_L$ referring to the full pulse duration with $T_L = 2\pi/\omega_L$ the laser period. A sufficient high spatiotemporal grid of $\Delta x/\lambda_L = \Delta t/T_L = 0.00125$ is used to resolve possible high frequencies of the scattered light. For the sake of comparison, the plasma electrons are initialized with either a cold or thermal start, and concerning the thermal case, an isotropic temperature of T_e =20eV is used, which is sufficient to mimic the field ionization induced by the laser prepulses.

Figure 1(b) and 1(c) show the first density crest at different time as approaching the end of the up-ramp. As described in Ref. [15], the wave crest narrows, develops into overcritical densities as propagating into denser regions and finally breaks around $x = 94\lambda_L$ shortly before the profile center. The central new feature is that the crest profiles show nearly the same characteristics regardless of introducing certain initial temperature. They can grow into ultrashort spikes of densities as high as $3n_c$ before breaking. In the present simulation, it takes about $10T_L$ for the crest density to grow from 0.25 to $3n_c$, which thereby provides a sufficient long time for colliding with a second probe laser. The overcritical mirror density is actually hard to implement in underdense plasmas.

Figure 1(d) further counts the corresponding γ_x spectra for the crest electrons obtained from the thermal case. A monoenergetic peak almost fixed at $\gamma_x = 3.8$ before breaking is achieved for this strong driver. The peaked spectrum appears to be consistent with that from highly nonlinear cold plasmas [10], indicating a fine mitigation of thermal wave-breaking due to the ramped profile. Such a high γ_x is close to, or even higher than, γ_p related to the phase velocity of the wakefield in a uniform plasma at the local density with the same drive laser. The wave crests before wave-breaking can be used to serve as perfect mirrors with appealing features such as overcritical concentrations, ultrashort durations, and peaked spectra. Most critically, these results can be obtained in thermal plasmas. The Doppler factors can extend over a few tens folds with the upshifted spectrum peaked around $\Gamma = 4\gamma_x^2 \approx 58$. Note that this high-frequency spectrum locates right in the XUV region, and can be achieved here with much lower driver intensity as compared to the laser-foil schemes[4]. This is because the mirror electrons attain forward-going momenta from the plasma wave motion rather than direct laser accelerations.

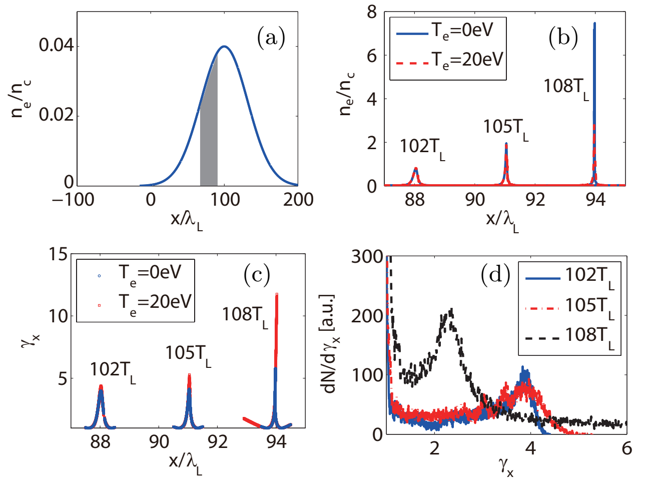

FIG. 1. (Color online) (a) The initial electron density profile with the gray color showing the favorable region for creating efficient and thermal-insensitive mirrors. (b) The first density crest of the wake wave at different time when approaching the end of the ramp for initially either a cold (blue-solid line) or thermal (red-dashed line) plasma. (c) Phasespace distributions of γ_x-x for the density spike electrons at corresponding time in (b). (d) γ_x-spectra for the density spike electrons at corresponding times in (b) for the thermal case.

In the following, we check the performance of the relativistic mirrors in coherent scattering of a probe laser incident from the right side. The probe laser is linearly polarized along y axis so as to distinguish it readily from the driver. It shares the same temporal envelope with the driver, and has a duration of $10T_L$ and an amplitude $a_p = 0.005$, which is just weak enough as not to induce significant nonlinear dynamics on the mirror electrons. The probe pulse is fine adjusted so that its center meets the first wake spike at $t = 105T_L$, i.e., the gray-

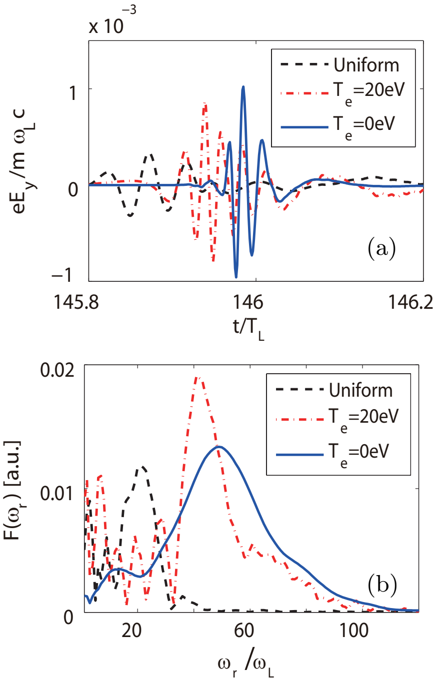

FIG. 2. (Color online) (a) The spatial profiles of the coherently scattered pulses obtained from the up-ramp tailored plasma [either with (red dot-dashed line) or without (blue solid line) initial electron temperature] or from a purely uniform thermal plasma (blue dashed line). (b) The corresponding frequency spectra for the pulses shown in (a).

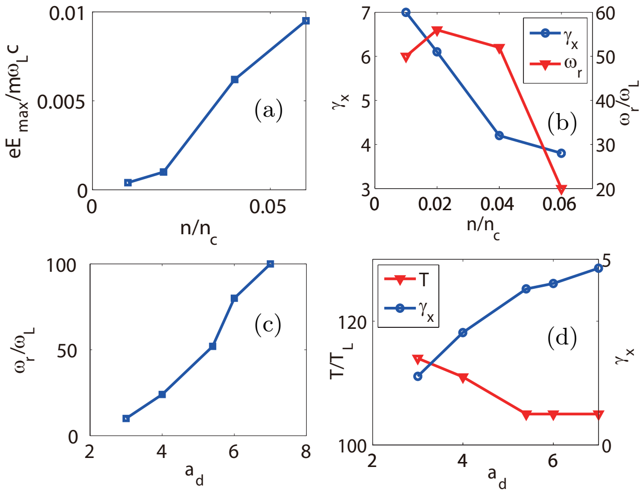

FIG. 3. (Color online) (a) The amplitude of the scattered pulse, (b) the monoenergetic part of γ_x before breaking (blue dots) and central frequency of the scattered spectra (red triangle) obtained with different n_0. (c) The central frequency of the scattered spectra obtained with different a_d. (d) The time instant of wave-breaking (red triangle) and the monoenergetic part of γ_x (blue circle) recorded at different a_d. All the simulations are performed with finite thermal temperature of $T_e = 20eV$.

colored region shown in Fig. 1(a). Figure 2 presents the reflected pulses and corresponding frequency spectra. We find quite similar results have been obtained for both cold and thermal cases, indicating the generation of temperature-insensitive mirrors in the present configuration. The reflectivity of the electric fields exceeds 2%, corresponding to energy conversion efficiency around 10^{-5}, higher than those obtained from underdense plasmas if thermal motion was included. The scattered spectra show a monochromatic peak around $42\omega_L$ corresponding to $\gamma_x \simeq 3.3$, which is in reasonable agreement with the above estimations. A slight downshifts of the spectra may be caused by the interaction with the probe pulse.

In order to further elucidate the unique role played by the up-ramp, we conduct simulations by having pulse collision in a purely uniform plasma with initial temperautre of 20eV and the same density $0.04n_c$ for comparison. We need to carefully choose a relatively lower-intensity driver so that the plasma wave can be driven very close to wavebreaking, but not involving fast breakdown due to premature thermal injection. A short Gaussian density ramp is also attached at the front to avoid breakdown by the sharp vacuum-plasma interface [17]. We therefore picked $a_d = 4$, and the results are shown by the blue dashed curve in Fig. 2. We find, however, much weaker scattering together with a shifted spectrum significantly below the up-ramp tailored cases. This deviation is arising from the fact that $a_d = 4$ is actually still not sufficient to drive to $\gamma_x = 3.8$ in this uniform but thermal plasma, and it's the thermal effects that prevent us from using higher-intensity drivers.

We find the present scheme is valid for a wide range of laser and plasma parameters. By changing the parameters, the resulting scatterings vary accordingly. The exact solution for wake excitation in an inhomogeneous plasma is hard to derive, but useful scaling dependence on the laser-plasma conditions can be well estimated. For this purpose, we simply characterize the plasma by a uniform plasma of density n_0. This is a reasonable assumption since the pulse collision indeed takes place near the end of the ramp within a short interval. Then all the relations derived for uniform plasmas can be used here. But one should bear in mind that these results found in inhomogeneous are robust against finite electron temperatures. For instance, higher n_0 would result in higher spike densities as indicated by the relation $n = n_0\beta_p/(\beta_p - \beta_e)$ with β_e the normalized fluid velocity of plasma electrons, thereby leading to enhanced reflectivity [18]. This is clearly shown in Fig. 3(a), where the amplitude of the scattered wave scales almost linearly with n_0. On the other hand, the Doppler-shifted spectrum is determined by γ_x of the spike electrons before breaking. For sufficient strong drivers, γ_p can be a good approximation for γ_x, and in the nonlinear regime it can be expressed as $\gamma_x \simeq \sqrt{\gamma_d} n_c/n_0$, where $\gamma_d = \sqrt{1 + a_d^2/2}$ is the normalized electron energy averaged over laser periods for a linearly polarized driver of strength a_d. Nonlinear laser evolution

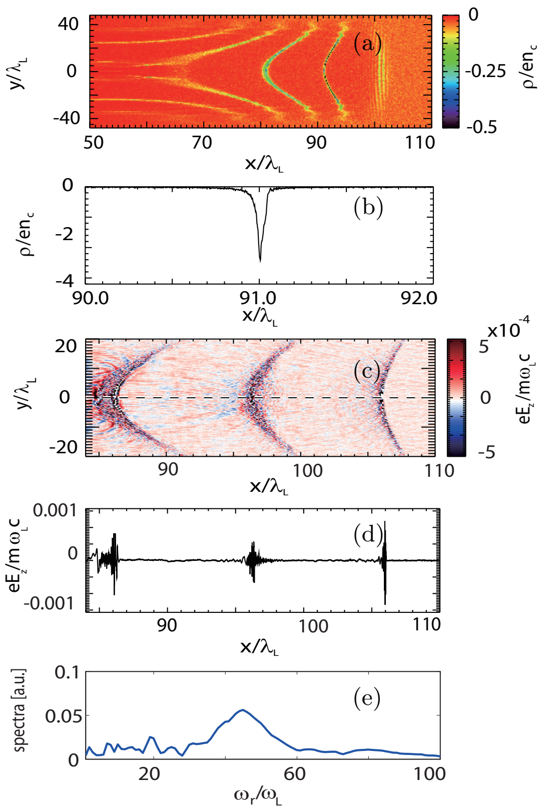

FIG. 4. (Color online) (a) 2D snapshot of the electron density at $t = 105T_L$ and (b) the corresponding lineout along $y = 0$ for the first wave crest. (c) 2D snapshot of the transverse electric fields E_z at $t = 125T_L$ and (d) the corresponding lineout along $y = 0$. (d) The frequency spectrum of the first scattered pulse.The initial temperature is set to be $T_e = 20eV$

[19] may lower this γ_x value, but should share the same scaling trend with a_d. In this sense, higher n_0 or weaker a_d will result in smaller γ_x, thereby a lower shifted spectrum, as corroborated in Fig. 3(b) and 3(d). While for low-intensity drivers (still with a_d >1), γ_x should mainly depend on the driver intensity, and a good approximation given by $\gamma_x \simeq (\gamma_d^4 - 1)/2\gamma_d^2$ for a square pump [20] can be used, which are again qualitatively confirmed by Fig. 3(c). Figure 3(d) further shows the time instant of wave-breaking driven at different a_d. Once a_d exceeds certain threshold (e.g. $a_d \sim 4.5$ for $n_0 = 0.04n_c$), this time instant will keep fixed around $t = 105T_L$ due to sharp wave-breaking [15].

Finally we examine the multi-dimensional effects using 2D PIC simulations. We have used a fairly large spot diameter of $34\lambda_L$ for the driver so as to preserve the 1D wake evolutions. Figure 4(a) shows 2D snapshot of the electron density at $t = 105T_L$, and Fig. 4(c) shows the scattered pulses at $20T_L$ later. As a comparison, the lineout plots of the density and scattered fields through $y = 0$ show nearly the same profiles and amplitudes with 1D cases. The multi-dimensional effects are mainly caused by the curved wake wavefronts, which arises due to the relativistic correction of the wave amplitude [21]. Another effect is the transverse-wake wave breaking [22], which can be more distinct in the present up-ramp density region, as seen in Fig. 4(a). Therefore, only the first few wake-wave crests can be used for relativistic mirrors in a practical multi-dimensional regime, while the subsequent wakes far behind will suffer from transverse breaking.

In conclusion, we have proposed a solution to overcome the thermal effects in the generation of relativistic mirrors from laser wakefields by using an up-ramp density profile. The ramped profile with proper gradient allows driving the wakefield with high intensity lasers and, at the same time, suppresses the premature thermal wave-breaking efficiently. The wake waves propagating near the end of the up-ramp are identified with overcritical density and monoenergetic spectrum. Enhanced pulse scattering has been extracted from multi-dimensional PIC simulations as compared to that in uniform but thermal plasmas. The present scheme works for a wide range of parameter space, and may pave a way toward efficient attosecond XUV radiations with a compact setup operated at high repetition rates.

This work is supported by the National Basic Research Program of China (under Grants No. 2013CBA01501 and 2013CBA01504), MOST international collaboration project (under Grant No. 0S2013GR0050), and the National Science Foundation of China (under Grants No. 11121504, 11374210, and 11205101).

[1] H. Daido, Reports on Progress in Physics **65**, 1513 (2002).
[2] S. V. Bulanov, T. Z. Esirkepov, M. Kando, A. S. Pirozhkov, N. N. Rozanov, *et al.*, Physics-Uspekhi **56** (2013).
[3] V. V. Kulagin, V. A. Cherepenin, M. S. Hur, and H. Suk, Physical review letters **99**, 124801 (2007).
[4] D. Kiefer, M. Yeung, T. Dzelzainis, P. Foster, S. Rykovanov, C. L. Lewis, R. Marjoribanks, H. Ruhl, D. Habs, J. Schreiber, *et al.*, Nature communications **4**, 1763 (2013).
[5] S. V. Bulanov, T. Esirkepov, and T. Tajima, Physical review letters **91**, 085001 (2003).
[6] M. Kando, Y. Fukuda, A. Pirozhkov, J. Ma, I. Daito, L.-M. Chen, T. Z. Esirkepov, K. Ogura, T. Homma, Y. Hayashi, *et al.*, Physical review letters **99**, 135001 (2007).
[7] M. Kando, A. Pirozhkov, K. Kawase, T. Z. Esirkepov, Y. Fukuda, H. Kiriyama, H. Okada, I. Daito, T. Kameshima, Y. Hayashi, *et al.*, Physical review letters **103**, 235003 (2009).
[8] M. Lobet, M. Kando, J. K. Koga, T. Z. Esirkepov, T. Nakamura, A. S. Pirozhkov, and S. V. Bulanov, Physics Letters A (2013).

[9] A. Solodov, V. Malkin, and N. Fisch, Physics of plasmas **13**, 093102 (2006).

[10] S. Bulanov, N. Naumova, F. Pegoraro, and J. Sakai, Physical Review E **58**, R5257 (1998).

[11] K. Schmid, A. Buck, C. M. Sears, J. Mikhailova, R. Tautz, D. Herrmann, M. Geissler, F. Krausz, and L. Veisz, Physical Review Special Topics-Accelerators and Beams **13**, 091301 (2010).

[12] Z.-M. Sheng, K. Mima, J. Zhang, and H. Sanuki, Physical review letters **94**, 095003 (2005).

[13] T. Katsouleas, Physical Review A **33**, 2056 (1986).

[14] P. Sprangle, J. Penano, B. Hafizi, R. Hubbard, A. Ting, D. Gordon, A. Zigler, and T. Antonsen Jr, Physics of Plasmas **9**, 2364 (2002).

[15] F. Li, Z. Sheng, Y. Liu, J. Meyer-ter Vehn, W. Mori, W. Lu, and J. Zhang, Physical review letters **110**, 135002 (2013).

[16] R. Fonseca, L. Silva, F. Tsung, V. Decyk, W. Lu, C. Ren, W. Mori, S. Deng, S. Lee, T. Katsouleas, *et al.*, (2002).

[17] S. Bulanov, I. Inovenkov, N. Naumova, and A. Sakharov, Sov. J. Plasma Phys **16**, 444 (1990).

[18] H.-C. Wu and J. Meyer-ter Vehn, The European Physical Journal D **55**, 443 (2009).

[19] C. B. Schroeder, C. Benedetti, E. Esarey, and W. Leemans, Physical Review Letters **106**, 135002 (2011).

[20] V. Berezhiani and I. Murusidze, Physics Letters A **148**, 338 (1990).

[21] A. Akhiezer and R. Polovin, Soviet Phys. JETP **3** (1956).

[22] S. Bulanov, F. Pegoraro, A. Pukhov, and A. Sakharov, Physical review letters **78**, 4205 (1997).